

## Spin-dependent resonant tunneling through semimetallic ErAs quantum wells in a magnetic field

A. G. Petukhov

*Physics Department, South Dakota School of Mines and Technology, Rapid City, South Dakota 57701-3995*

W. R. L. Lambrecht and B. Segall

*Department of Physics, Case Western Reserve University, Cleveland, Ohio 44106-7079*

(Received 19 October 1995)

Resonant tunneling through semimetallic ErAs quantum wells embedded in GaAs structures with AlAs barriers was recently found to exhibit an intriguing behavior in magnetic fields: a peak splitting occurred only in fields perpendicular to the film while a second resonant channel opened for in-plane fields. The behavior is explained in terms of the valence-band states in ErAs in the vicinity of the  $\Gamma$  point, their exchange splitting induced by the localized Er  $4f$  magnetic moments, and by a selection rule involving the total angular momentum component along the normal to the interface.

The utilization of thin metallic layers as active components in semiconductor devices such as metal base and resonant tunneling transistors opens new avenues in microelectronics. Resonant tunneling through thin metallic layers embedded in a semiconductor has been reported by several authors.<sup>1</sup> A promising materials system for the study of this phenomenon is semimetallic ErAs embedded in GaAs since the two are closely lattice matched.<sup>2</sup> Because of the open  $4f$  shell of erbium, these heterostructures also have interesting magnetic behavior.<sup>3-9</sup> Here we provide a theoretical explanation for the unusual behavior of resonant tunneling through ErAs layers in magnetic fields of different orientation, which was recently reported by Brehmer *et al.*<sup>3</sup> and Zhang *et al.*<sup>4</sup> These experiments were carried out on resonant tunneling diode (RTD) structures consisting of ErAs quantum wells and AlAs barriers sandwiched between the  $n+$  doped GaAs substrate and GaAs capping layers.

The measurements of differential conductance ( $dI/dV$  vs  $V$ ) (Ref. 3) indicate the presence of two different resonant tunneling channels called  $A$  and  $B$ . The peak  $A$  splits in a magnetic field perpendicular to the layers, but remains nearly unaffected (slightly shifted) by a magnetic field parallel to the layers. The  $B$  channel, on the other hand, shows no observable splitting for either direction of the field, is only weakly resolved as a shoulder in zero or perpendicular field, but is strongly enhanced by a field parallel to the film. The most extensive results and the ones we focus on here were obtained for the  $[113]$  orientation of the film. However, similar results were obtained for other orientations of the films. That indicates that the phenomena are not determined by specific intrinsic crystallographic directions but rather by the relative orientation of field and interface.

In the present paper, we will show that this behavior is explained by tunneling of electrons into the ErAs light and heavy-hole states in the vicinity of the  $\Gamma$  point for the  $A$  and  $B$  resonances, respectively. In the absence of a magnetic field or in a perpendicular field, tunneling is predominantly only into the light-hole bands because of an approximate conservation of the total angular (orbital and spin) momentum component along the normal of the film. The exchange splitting of these states induced by coupling to the open  $4f$  shell leads

to an anomalously large Zeeman splitting. On the other hand, a parallel field allows for tunneling into the heavy-hole band leading to an enhancement of channel  $B$ . The splitting in this case will be shown to be reduced.

To understand the tunneling behavior, a detailed understanding of the ErAs band structure and magnetic properties is required. This is provided by our recent electronic structure calculations<sup>8,9</sup> of ErAs and related  $\text{Er}_x\text{Sc}_{1-x}\text{As}$  alloys, the results of which were in good agreement with magnetotransport measurements.<sup>7</sup> The first question to be addressed is whether the tunneling takes place into the conduction (electron) or valence (hole) states. This is expected to depend on the film direction. For the  $[113]$  direction under consideration, the band structure (see Fig. 1) shows clearly that unoccupied electron states are more than 1.5 eV above the Fermi level. Hence they cannot be involved in the tunneling. In fact, although the Schottky barrier height at the ErAs/AlAs interface is presently unknown, the Fermi level in the ErAs must line up with the donor states near the conduction band edge deep in the  $n+$  doped GaAs region. Implicit in the above argument is that  $k_{\parallel}$  is conserved in the resonant tunneling and that only electrons with  $k_{\parallel} \approx 0$  are involved in the transport from GaAs because the conduction-band minimum in GaAs is at  $\Gamma$ .

Using the simple infinite barrier model, a first estimate can be obtained for the quantum confined states in the ErAs quantum well. For a film thickness of  $N$  monolayers (ML), there are  $n=1, \dots, N$  quantized values of wave vector  $k_{\perp, n} = n\pi/Na_{\perp}$ , where  $a_{\perp}$  is the distance between two monolayers. The corresponding values of  $k_{\perp}$  are indicated as vertical lines in Fig. 1 for a layer thickness of 12 ML. This shows that only the  $n=1$  quantized hole states lie close to the Fermi level and are likely to be involved in the tunneling.

To relate these quantized energies  $E_n$  to the voltages  $V$  at which resonance occurs, we need to know the voltage profile in the RTD. This is somewhat uncertain because the top and bottom interfaces of ErAs are of different quality due to difficulties in the epitaxial overgrowth on ErAs. For a symmetric structure, there would be equal voltage drops across the two insulating GaAs space charge layers and AlAs barriers, leading to a resonance when  $V/2 \approx E_n$ . Direct measurements of the voltage drop on three terminal devices, however, have

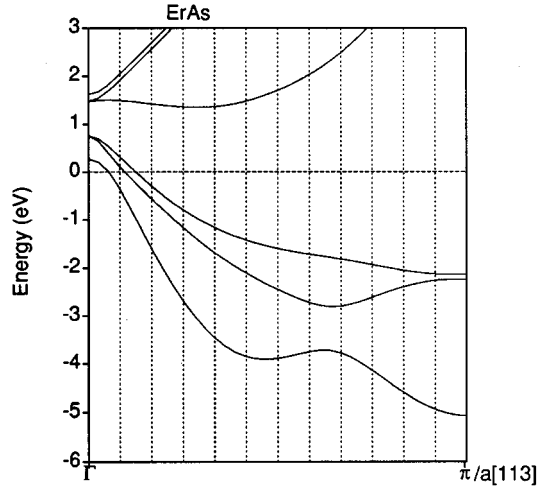


FIG. 1. Energy band structure of ErAs along the [113] direction in zero field. The vertical lines indicate quantized  $k_{\perp,n}$  values in an infinite barrier quantum well of 12 ML.

shown that most of the voltage drop occurs on the substrate to ErAs interface.<sup>3</sup> This implies that  $E_n \approx V$ .

Unlike our earlier calculations,<sup>8</sup> the band structure shown in Fig. 1 includes the effect of spin-orbit coupling, which, as will be shown below, is essential for understanding the magnetic field dependence. Otherwise, the details of the calculation method are similar to those of Ref. 8. The calculations are performed within the atomic-sphere approximation of the linear muffin-tin orbital method<sup>10</sup> and are based on local spin density functional theory. The spin-orbit coupling terms are added as a perturbation to the spin-dependent Hamiltonian, which is then diagonalized numerically without further approximations.<sup>10</sup> The spin polarization arises from the alignment of unpaired spins in the  $4f$  level, which is treated as an open shell corelike level without dispersion. In the absence of a magnetic field, the  $4f$  localized spin magnetic moments are randomly oriented and the bands are described by a calculation without spin polarization.

The manifold of valence states around  $\Gamma$  can be described by the Kohn-Luttinger (KL) Hamiltonian,<sup>11</sup> which accounts for the behavior up to quadratic terms in  $\mathbf{k}$ . In the following, we use this Hamiltonian in the spherical approximation (i.e.,  $\gamma_2 = \gamma_3$  in terms of the conventional Luttinger parameters<sup>11</sup>) in order to gain a qualitative understanding of the magnetic field effects. We stress, however, that this description of the nature of the quantum states involved in the tunneling and the associated conservation laws remain approximately valid even in the complete calculation. The KL Hamiltonian we start from is

$$H = -(\gamma_1 + 4\gamma_2)\mathbf{k}^2 + 6\gamma_2(\mathbf{L} \cdot \mathbf{k})^2 + [\lambda_0 + \lambda_1\mathbf{k}^2 + \lambda_2(\mathbf{L} \cdot \mathbf{k})^2](\mathbf{S} \cdot \hat{\mathbf{B}}) + \frac{2}{3}\Delta_{\text{SO}}\left(\mathbf{L} \cdot \mathbf{S} - \frac{1}{2}\right), \quad (1)$$

where  $\mathbf{L}$  is the  $l=1$  orbital momentum operator describing  $p$ -like hole states at the top of the valence band of ErAs,  $\mathbf{S}$  is

the spin operator, and  $\hat{\mathbf{B}}$  a unit vector along the magnetic field. The first two terms are the usual Luttinger terms.<sup>11</sup> The last term is the spin-orbit coupling term with the  $1/2$  inside the parentheses being a reference-level shift to the valence-band maximum. The parameters  $\lambda_i$  describe the splitting of the valence states in the presence of a magnetic field. Here the splitting is primarily due to the exchange interaction of the holes with the ferromagnetically aligned localized moments of  $4f$  electrons. The alignment of the latter is well described by standard Brillouin theory of paramagnets.<sup>6</sup> In our numerical calculations we assume saturated spin polarization. This is valid because the measurements were taken at  $T=4$  K and the applied magnetic field was 8 T.<sup>6</sup> Direct coupling of the angular momentum to the magnetic field (the Zeeman effect) is neglected as it is much smaller than the coupling to the exchange field. Also neglected are the terms that lead to the formation of Landau levels. The above Hamiltonian is thus equivalent to the one used in our first-principles calculations and its parameters can be extracted from the latter.

For reasons already explained above, we can now set  $k_{\parallel}=0$  and choose the  $z$  axis along the normal to the interface. The quantization of  $k_{\perp}$  in the infinite barrier model then fixes the  $\mathbf{k}$  completely. In the absence of the spin-orbit interaction the above Hamiltonian (1) describes two sets of spin-polarized bands that are independent of the direction of the magnetic field. The spin-orbit interaction now couples the spin direction (determined by the magnetic field) to the orbital angular momentum direction (fixed by  $k_{\perp}$  to be normal to the interface). This is what leads to the nontrivial magnetic-field orientation dependence. More precisely, without the magnetic-field term but including spin-orbit interaction the Hamiltonian commutes with  $J_z$  where  $J_z = L_z + S_z$  is the projection of the total angular momentum onto the direction normal to the interface. If the magnetic field is along the same direction ( $\mathbf{B} \parallel \hat{\mathbf{z}}$ ), the Hamiltonian (1) maintains this cylindrical symmetry and splits up into two  $2 \times 2$  submatrices  $H_{n,\pm 1/2}^{\perp} - E_n^0$ , describing the coupling between the  $|3/2, \pm 1/2\rangle$  and  $|1/2, \pm 1/2\rangle$  states,

$$\begin{pmatrix} (1/6)(2A_n \pm B_n \mp C_n) & (\sqrt{2}/6)(2A_n \mp 2B_n \mp C_n) \\ (\sqrt{2}/6)(2A_n \mp 2B_n \mp C_n) & (1/6)(4A_n \pm B_n \pm 2C_n) - \Delta_{\text{SO}} \end{pmatrix}, \quad (2)$$

where  $E_n^0 = -(\gamma_1 + 4\gamma_2)k_{\perp,n}^2$ ,  $A_n = 6\gamma_2k_{\perp,n}^2$ ,  $B_n = \lambda_0 + \lambda_1k_{\perp,n}^2$ , and  $C_n = \lambda_2k_{\perp,n}^2$ . We will primarily be concerned with  $n=1$  states. Similarly the eigenvalues of the  $|3/2, \pm 3/2\rangle$  states are

$$E_{n,\pm 3/2} = E_n^0 + A_n \pm D_n/2, \quad (3)$$

where  $D_n = B_n + C_n$ .

In the case of the magnetic field parallel to the interface,  $J_z$  no longer commutes with the Hamiltonian and there is an additional mixing of the eigenstates of the original Hamiltonian (without field). The energy spectrum of the quantum well can, however, be found as the eigenvalues of the two  $3 \times 3$  submatrices  $H_{n,\pm}^{\parallel} - E_n^0$ , written in the basis  $(1/\sqrt{2})(|3/2, 3/2\rangle \pm |3/2, -3/2\rangle)$ ,  $(1/\sqrt{2})(|3/2, 1/2\rangle \pm |3/2, -1/2\rangle)$ , and  $(1/\sqrt{2})(|1/2, 1/2\rangle \mp |1/2, -1/2\rangle)$

$$\begin{pmatrix} A_n & \pm(1/\sqrt{12})D_n & \pm(1/\sqrt{6})D_n \\ \pm(1/\sqrt{12})D_n & (1/3)(A_n \pm B_n) & (\sqrt{2}/6)(2A_n \mp B_n) \\ \pm(1/\sqrt{6})(D_n) & (\sqrt{2}/6)(2A_n \mp B_n) & (1/6)(4A_n \pm B_n) - \Delta_{SO} \end{pmatrix}. \quad (4)$$

The analysis of the structure of the matrices (2)–(4) allows one to explain semiquantitatively all the features of the resonant tunneling experiments in a magnetic field. First, we recall that the electrons tunneling from the  $n^+$  GaAs conduction-band minimum are  $s$ -like and have  $M_J = \pm 1/2$ . With the magnetic field absent or perpendicular to the layers,  $M_J$  is a good quantum number that must be (approximately) conserved. Hence tunneling transitions between states with  $|M_J| = 1/2$  and  $|M_J| = 3/2$  are forbidden. This explains why in that case only the  $A$  channel (corresponding to tunneling into the light-hole states with  $M_J = \pm 1/2$ ) is pronounced. The small shoulder of the  $B$  channel is due to the fact that in the real band structure the axial symmetry is slightly broken. For parallel fields, the  $M_J$  states are mixed and the  $B$  channel becomes available for tunneling. The observed splitting in the perpendicular magnetic field is also easily understood since the energies depend on the sign of  $M_J$ . The magnetic-field dependence of this splitting was shown by Zhang *et al.*<sup>4</sup> to follow the Brillouin theory of paramagnetic alignment of localized spins as expected in the present theory.

Figures 2(a) and 2(b) show the eigenvalues of the above matrices in perpendicular and in-plane field, respectively, with the parameters  $E_n^0 = -84.3k_\perp^2$ ,  $A_n = 59.7k_\perp^2$ ,  $B_n = -9.75k_\perp^2$ ,  $C_n = 14k_\perp^2$ , with  $k_\perp$  in units  $\pi/a_\perp$  and  $\Delta_{SO} = 0.45$  and all energies in eV. These parameters were extracted from our first-principles calculations and appropriately adjusted for the spherical approximation. The small spin splitting at  $\Gamma$ ,  $\lambda_0 \approx 1$  meV was neglected. As discussed in our previous work,<sup>8</sup> the Fermi-level position was slightly shifted from its local-density approximation (LDA) value as it was found that the LDA overestimates the Fermi surface volume<sup>8</sup> because of the neglect of electron interaction self-energy effects. This figure clearly shows that the light hole spin splitting is about 5 times larger for the perpendicular than for the in-plane field. Also indicated in this figure are the experimental resonance positions for varying thicknesses (i.e., different  $k_{\perp,n}$ ) assuming  $V = E_n$ . Overall, the agreement is quite good for the absolute energies of the resonances, the dispersions, and the splitting between light and heavy hole. The spin splitting appears to be slightly underestimated in the calculation. Experimentally the splitting was seen to be about 80 meV, while the model gives 50 meV.

The advantage of the present analytical model is that we can easily investigate the effect of varying parameters. Because spin-orbit interaction is fairly large, the coupling to the spin-orbit split-off bands can be treated in perturbation theory. Up to first order terms in  $1/\Delta_{SO}$ , the light hole spin splitting in perpendicular field is  $\Delta_{xc}^\perp(\text{lh}) \approx (B_n - C_n)/3 - 4A_n(2B_n + C_n)/9\Delta_{SO}$ , which is of order 50 meV, while for the in-plane field, it is:  $\Delta_{xc}^\parallel(\text{lh}) \approx 2B_n/3 - 4A_nB_n/9\Delta_{SO}$ , which is of order 10 meV. Similarly, we find that the heavy-hole splitting for the in-plane field up to terms in  $1/\Delta_{SO}$  is

zero, which explains why no spin splitting is observed for the  $B$  channel. For the perpendicular field, the heavy-hole splitting is  $B_n + C_n \approx 40$  meV, but is not observed because in that case this channel is reduced to a weak shoulder on a rising background. Again up to the same order in  $1/\Delta_{SO}$ , the component of the allowed  $J = 1/2$  channel in the light-hole eigenstate for in-plane field is given by  $\{1 - [(D_n/\sqrt{12})(1 + 2A_n/\Delta_{SO})/(2A_n/3)]^2\}^{1/2}$ , which is about 94%. This is consistent with the fact that the  $A$  channel is not noticeably reduced in intensity when the in-plane field is switched on.

A quantitative calculation of resonance intensity for the  $B$  channel due to the weak breaking of axial symmetry and its gradual switching on in the magnetic in-plane field will require a more detailed study of the quantum tunneling process. Finally, we note that the resonances in this system are relatively broad compared to typical resonant tunneling in semiconductor quantum wells. Among other broadening mechanisms, this may result from the loosening of  $k_\parallel$  conservation due to the roughness of the top layer interface. We thus anticipate that with further improvements in the material some of the finer details of our model may be checked experimentally in future work.

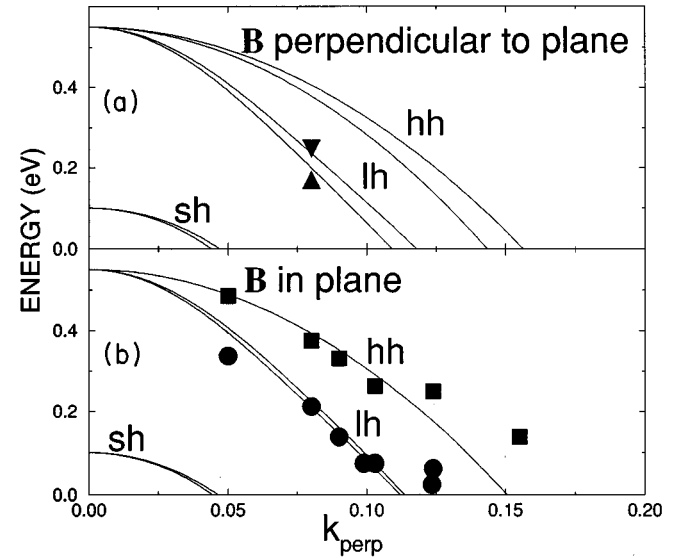


FIG. 2. Band structure of ErAs near the valence-band maximum in the  $[113]$  direction in a saturating magnetic field which in (a) is perpendicular and in (b) is parallel to the  $(113)$  plane within the spherical Kohn-Luttinger model. Experimental resonance positions given by  $V = E_n$  (see text) for  $n = 1$  and different film thicknesses (or  $k_{\perp,n}$  values) are indicated by circles for the  $A$  channel and squares for the  $B$  channel. The experimental spin-split  $A$ -channel resonances are indicated by triangles for one layer thickness in (a). The heavy-hole (hh), light-hole (lh), and split-off hole (sh) bands are labeled.

We have also carried out fully first-principles calculations of the bands in the [113] direction in parallel and perpendicular magnetic field including the spin-orbit coupling. These calculations qualitatively confirm the above results, but lead to a somewhat smaller light-hole spin splitting (30 meV) in perpendicular field than the spherical model (which was already too small) and slightly lower masses and hence slightly lower level positions for a given layer thickness. A possible origin for this discrepancy is that our present calculations are based entirely on bulk band structures and infinite wall quantization. In the finite wall quantum wells, i.e., taking into account the actual interface electronic structure, mixing of Er 5*d* derived bands, which have larger spin splitting, into the relevant hole states is expected to occur and may lead to a substantial enhancement of the exchange splitting effects.

In conclusion, the spherical Kohn-Luttinger model of the valence-band maximum supplemented with a strongly enhanced spin Zeeman effect (due to coupling of the valence electrons with the localized magnetic moments of the 4*f* electrons, which are aligned in the field) provides a good

semiquantitative description of the ErAs valence-band maximum and its associated eigenstates. The tunneling behavior can be understood in terms of approximate conservation of the total angular momentum component along the normal to the interface. For perpendicular or zero field this forbids the transitions into the heavy-hole bands while the latter become allowed by mixing of states for an in-plane field. The origin of this approximate selection rule is that the  $k_{\parallel} \approx 0$  of the electrons originating in the GaAs conduction band is conserved. This in turn fixes the quantization axis for the orbital angular momentum along the normal to the interface. The spin direction on the other hand is fixed by the magnetic field. The spin-orbit coupling is thus essentially responsible for the qualitatively different behavior of the tunneling in the parallel and perpendicular fields.

We wish to thank S. J. Allen and D. E. Brehmer for stimulating discussions. This work was supported by the Air Force Office of Scientific Research Grant No. F49620-95-1-0043 and by the National Science Foundation under Grant No. OSR-9108773 and the South Dakota Future Fund.

<sup>1</sup>N. Tabatabaie, T. Sands, J. P. Harbison, H. L. Gilchrist, and V. G. Keramidis, *Appl. Phys. Lett.* **53**, 2528 (1988), and references therein.

<sup>2</sup>C. J. Palmström, N. Tabatabaie, and S. J. Allen, Jr., *Appl. Phys. Lett.* **53**, 2608 (1988); C. J. Palmström, S. Mounier, T. G. Finstad, and B. Miceli, *ibid.* **56**, 382 (1990).

<sup>3</sup>D. E. Brehmer, Kai Zhang, Ch. J. Schwarz, S.-P. Chau, S. J. Allen, J. P. Ibbetson, J. P. Zhang, C. J. Palmström, and B. Wilkens, *Appl. Phys. Lett.* **67**, 1268 (1995).

<sup>4</sup>Kai Zhang, D. E. Brehmer, S. J. Allen, Jr., and C. H. Palmström, in *Proceedings of the 21st International Symposium on Compound Semiconductors, San Diego, 1994*, edited by H. Gorankin and U. K. Mishra, IOP Conf. Proc. No. 141 (Institute of Physics, Bristol, 1995), pp. 845–850.

<sup>5</sup>S. J. Allen, Jr., N. Tabatabaie, C. J. Palmström, G. W. Hull, T. Sands, F. DeRosa, and H. L. Gilchrist, *Phys. Rev. Lett.* **62**, 2309 (1989).

<sup>6</sup>S. J. Allen, Jr., F. DeRosa, C. J. Palmström, and A. Zrenner, *Phys. Rev. B* **43**, 9599 (1991).

<sup>7</sup>R. Bogaerts, L. Van Bockstal, F. Herlach, F. M. Peeters, F. DeRosa, C. J. Palmström, and S. J. Allen, Jr., *Physica (Amsterdam)* **177B**, 425 (1992); **184**, 2320 (1993).

<sup>8</sup>A. G. Petukhov, W. R. L. Lambrecht, and B. Segall, *Phys. Rev. B* **50**, 7800 (1994).

<sup>9</sup>A. G. Petukhov, W. R. L. Lambrecht, and B. Segall, *Phys. Rev. B* (to be published).

<sup>10</sup>O. K. Andersen, *Phys. Rev. B* **12**, 3060 (1975).

<sup>11</sup>J. M. Luttinger, *Phys. Rev.* **102**, 1030 (1956).